ORIGINAL ARTICLE

Journal of Cachexia, Sarcopenia and Muscle 2021; **12**: 2199–2210
Published online 17 October 2021 in Wiley Online Library (wileyonlinelibrary.com) **DOI:** 10.1002/jcsm.12830

Skeletal muscle atrophy-induced hemopexin accelerates onset of cognitive impairment in Alzheimer's disease

Tsukasa Nagase and Chihiro Tohda*

Section of Neuromedical Science, Division of Bioscience, Institute of Natural Medicine, University of Toyama, Toyama, Japan

Abstract

Background Alzheimer's disease (AD) is an unmet medical need worldwide, and physical inactivity is a risk factor for AD. Performing physical exercise is difficult at old age, and thus, decline in physical movement may be a cause of age-associated lowering of the brain function. This study aimed to elucidate the molecular mechanism and onset of the skeletal muscle atrophy-induced acceleration of AD.

Methods Pre-symptomatic young 5XFAD or non-transgenic wildtype mice were used. The bilateral hindlimbs were immobilized by placing them in casts for 14 days. Cognitive function was evaluated using the object recognition and spatial memory tests. Further, the hindlimb muscles were isolated for organ culture. Conditioned media (CM) of each muscle was separated by two-dimensional polyacrylamide gel electrophoresis (2D-PAGE). Protein expressions in the CM were analysed by matrix-assisted laser desorption/ionization-time-of-flight mass spectrometry analysis. The expression levels of candidate proteins were quantified using ELISA. After continuous intracerebroventricular (i.c.v.) infusion of recombinant hemopexin, cognitive function was evaluated. Gene microarray analysis of the hippocampus was performed to investigate the molecules involved in the accelerated memory deficit. Real-time reverse transcription polymerase chain reaction and histological analysis confirmed the expression.

Results Casting for 2 weeks reduced skeletal muscle weight. Object recognition memory in the cast-attached 5XFAD mice ($n = 7$, training vs. test, $P = 0.3390$) was impaired than that in age-matched wildtype ($n = 7$, training vs. test, $P = 0.0523$) and non-cast 5XFAD mice ($n = 7$, training vs. test, $P = 0.0473$). On 2D-PAGE, 88 spots were differentially expressed in muscle CM. The most increased spot in the cast-attached 5XFAD CM was hemopexin. Hemopexin levels in the skeletal muscle ($n = 3$, $P = 0.0064$), plasma ($n = 3$, $P = 0.0386$), and hippocampus ($n = 3$, $P = 0.0164$) were increased in cast-attached 5XFAD mice than those in non-cast 5XFAD mice. Continuous i.c.v. infusion of hemopexin for 2 weeks induced memory deficits in young 5XFAD mice ($n = 4$, training vs. test, $P = 0.6764$). Lipocalin-2 (*Lcn2*) messenger RNA (mRNA), neuroinflammation-associated factor, was increased in the hippocampus in hemopexin-infused 5XFAD mice than in control mice. LCN2 protein in the hippocampus was localized in the neurons, but not glial cells. *Lcn2* mRNA levels in the hippocampus were also increased by cast-immobilization of the hindlimbs ($n = 6$, $P = 0.0043$).

Conclusions These findings provide new evidence indicating that skeletal muscle atrophy has an unbeneficial impact on the occurrence of memory impairment in young 5XFAD mice, which is mediated by the muscle secreted hemopexin.

Keywords Muscle atrophy; Memory deficit; Alzheimer's disease; Dementia; Hemopexin; Neuroinflammation

Received: 4 August 2021; Revised: 8 September 2021; Accepted: 15 September 2021
**Correspondence to: Chihiro Tohda, Section of Neuromedical Science, Division of Bioscience, Institute of Natural Medicine, University of Toyama, Toyama 930-0194, Japan. Phone and Fax: +81-76-434-7646, Email: chihiro@inm.u-toyama.ac.jp*

Introduction

Alzheimer's disease (AD) is one of the most unmet medical needs worldwide. AD is pathologically defined as the presence of amyloid β (Aβ) deposition and neurofibrillary tangles in the brain. Gene mutations found in patients with familial AD facilitate Aβ production, which supports the Aβ hypothesis. As the overexpression of Aβ is a causal factor of AD, inhibiting the production and deposition of Aβ is considered as a therapeutic approach for AD.[1] However, except aducanumab, drug candidates in numerous clinical studies based on the Aβ theory have repeatedly failed to recover cognitive function.[2,3] Moreover, several studies indicate that there are aged individuals with Aβ in the brain showing little or no cognitive impairment.[4–7] Taken together, the roles of Aβ may be collateral or can modulate cognitive impairment, and that other factors may also be associated with the initiation and deterioration of the brain's function.

Several epidemiological studies suggest that traumatic brain injury, lifestyle-related disease, and smoking are major risk factors for AD.[8] However, risk-reducing factors, such as long education period and physical exercise, are also indicated. Age-associated muscle atrophy is known as sarcopenia. The relationship between sarcopenia and cognitive function has been shown to be negatively correlated by the cross-sectional study of healthy old men[9] and meta-analysis.[10] Regarding hospitalization-related disorders, a cross-sectional study of hospitalized aged adults investigating relationship between the prevalence of sarcopenia and cognitive impairment showed that the both of decrease in physical activity and cognitive decline were associated with hospitalization.[11,12] Although those studies suggest the relationship among aging, skeletal muscle atrophy, and cognitive decline, no obvious evidences show that skeletal muscle atrophy directly induces cognitive impairment. As physical exercise is difficult to perform with increasing age, we hypothesized that a decline in physical movement may be a cause of age-associated lowering of the brain function. A decline in physical exercise leads to the loss of skeletal muscle. We hypothesized that sarcopenia induced the onset of AD, and therefore, we aimed to clarify that the skeletal muscle atrophy triggered a decline in brain function in AD.

We hypothesized that some molecules traveling from the skeletal muscles to the brain may affect the brain function. The skeletal muscle is an endocrine organ that secretes several factors that are collectively called as myokines, including cytokines, peptides, and growth factors, to maintain homeostasis.[13,14] As a majority of myokines have autocrine and paracrine effects, even the distal organs can be affected by myokines. Several myokines, such as brain-derived neurotrophic factor, insulin-like growth factor-1, FNDC5/irisin, and cathepsin B are secreted by the skeletal muscles during exercise and are also increased in the brain.[15–17] These myokines have a beneficial effect on the neuronal function. However, myokines, that are not beneficial for brain function, secreted from the atrophied skeletal muscle, remain to be identified. Therefore, this study aimed to elucidate the phenomenon of the skeletal muscle atrophy-induced acceleration of AD onset and its molecular mechanism.

Methods

Animals

Transgenic mice (5XFAD) were obtained from Jackson Laboratory (Bar Harbor, ME, USA). The 5XFAD mice have the following five mutations: Swedish (K60N and M671L), Florida (I716V), and London (V717I) in human APP695 cDNA and human PS1 cDNA (M146L and L286V) under transcriptional control of the neuron-specific mouse Thy-1 promoter.[18] They were maintained by crossing hemizygous transgenic mice with B6/SJL F1 breeders. All animals were allowed *ad libitum* access to water and food and were maintained in a controlled environment (22 ± 2°C, 12 h light/dark cycle starting at 7:00 am). All animal experiments and protocols were performed in accordance with the Guidelines for the Care and Use of Laboratory Animals of the Sugitani Campus of the University of Toyama, Japan. The approval number for the animal experiment was A2020INM-1, and the confirmation number for the gene recombinant experiment was G2018INM-2. All efforts were made to minimize the number of animals used.

Induction of hindlimb muscle atrophy

Muscle atrophy was induced by immobilization of the hind limbs, as previously described.[19] All animals were anesthetized by intraperitoneal administration of a mixture of three anaesthetics: 0.75 mg/kg of medetomidine (ZENOAQ, Fukushima, Japan), 4.0 mg/kg of midazolam (Sandoz, Tokyo, Japan), and 5.0 mg/kg of butorphanol (Meiji Seika Pharma, Tokyo, Japan). Further, the hair was removed from the thigh to ankle. Next, ethylene propylene diene monomer rubber foam tape (Cemedine, Tokyo, Japan) was cut to approximately 3 cm, and the foam tape was loosely wrapped to extend the ankle joint. The foam was covered with a soft vinyl chloride insulating cap (TIC-22, Nichifu, Osaka, Japan) using double-sided tape.

The insulating cap was fastened by wrapping with a strong adhesive tape (Asahipen, Osaka, Japan), aluminium foil tape (Nichiban, Tokyo, Japan), and vinyl tape (Nitto, Osaka, Japan). A foam tape cut to approximately 1 cm was attached to the back of the knee, fixed in the extended position with cloth surgical tape (Nitoms, Tokyo, Japan), and covered with vinyl tape. The same amount of anti-anaesthetic was intraperitoneally administered, and the mice were allowed to stand on a hot plate at 37°C until awake.

Object recognition test

All tests were performed in a dim room (61 LUX). In an open field with a black floor and walls composed of polyvinyl chloride (30 cm × 40 cm × 36 cm height), two identical objects (A, A') that the mouse saw for the first time were placed at regular intervals. The number of contacts with each object was measured for 10 min (Training session). After an interval (1 h or 24 h), object A' was replaced with a novel object B, and the number of contacts with each object was measured for 10 min (Test session). The preference index (PI) was calculated as follows:

i Training session PI = (number of contacts to A' /total number of contacts) × 100
ii Test session PI = (number of contacts to B/total number of contacts) × 100

Object location test

In an open field, two identical objects (C1 and C2) that the mouse saw for the first time were placed at regular intervals. The number of contacts with each object was measured for 10 min (Training session). After 30 min, the position of one of the objects was moved, and the number of contacts with each object was measured for 10 min (Test session).

i Training session PI = (number of contacts to C2/total number of contacts) × 100
ii Test session PI = (number of contacts to C2/total number of contacts) × 100

Organ culture

Wildtype and 5XFAD mice with or without cast were anesthetized by intraperitoneal administration of a mixture of three anaesthetics, followed by UV irradiation and spraying with 70% ethanol. The skin of the hindlimbs was incised, and the tibialis anterior and triceps surae were isolated following cardiac perfusion with ice-cold saline. Insert cups (ADVANTEC, Dublin, CA, USA) were placed in 24-well plates containing myocyte growth medium (PromoCell, Heidelberg, Germany). The skeletal muscles were placed in an insert cup and cultured for 24 h. After culturing, the insert cup was removed, and all culture supernatants [conditioned media (CM)] were collected. The protein concentration of CM was quantified using a Pierce 660 nm Protein Assay Kit (Thermo Fisher Scientific, Rockford, IL, USA). Absorbance measurements were performed using a multimode plate reader (FilterMax F5; Molecular Devices, San Jose, CA, USA).

Two-dimensional polyacrylamide gel electrophoresis

Sodium dodecyl sulphate sample buffer (250 mM Tris–HCl pH 6.8, 8% sodium dodecyl sulphate, and 0.08% bromophenol blue) was added to the CM to adjust the protein concentration to 1 mg/mL, and incubated at 90°C for 5 min. The sample was separated (200 μg per sample) using two-dimensional polyacrylamide gel electrophoresis (2D-PAGE) (GENOMINE, Inc., Korea), and the separated proteins were stained by alkaline silver staining. Proteins whose levels increased in the cast CM were identified. The proteins were excised, digested with trypsin, mixed with α-cyano-4-hydroxycinnamic acid in 50% acetonitrile/0.1% trifluoroacetic acid, and subjected to matrix-assisted laser desorption/ionization-time-of-flight mass spectrometry analysis (Microflex LRF 20, Bruker Daltonics, Billerica, MA, USA).

Hemopexin levels in the skeletal muscle, plasma, and brain

Wildtype and 5XFAD mice with or without cast were anesthetized by intraperitoneal administration of a mixture of triple anaesthetics, followed by sterilization by UV irradiation and 70% ethanol. Blood was collected and centrifuged at 12 000*g* at 4°C for 10 min. The plasma was separated from the supernatant. After cardiac perfusion with ice-cold saline, the skin was incised, and the triceps surae and hippocampus were isolated. The muscles and hippocampus were homogenized with Mammalian Protein Extraction Reagent (M-PER, Thermo Fisher Scientific) containing protease and phosphatase inhibitor cocktail (Thermo Fisher Scientific). After standing on ice, the samples were centrifuged at 12 000*g* at 4°C for 15 min. The supernatant was collected and used as the lysate. The protein concentration was quantified using Pierce 660 nm Protein Assay Kit. Absorbance was measured using a multimode plate reader (FilterMAX F5). Hemopexin concentrations in the CM, muscle lysate, plasma, and hippocampus were quantified using ELISA according to the manufacturer's protocol of the Hemopexin Mouse ELISA Kit (Abcam, Cambridge, UK).

Gene microarray

The 5XFAD mice were continuously administered recombinant hemopexin or vehicle solution for two-weeks. After cardiac perfusion with ice-cold saline, the hippocampus was isolated. The hippocampus was homogenized with ISOGEN II (Nippon Gene, Tokyo, Japan), and the supernatant was collected. RNA was precipitated with isopropanol, and the precipitate was dried. Thirty microlitres of RNase-free water was added to the RNA precipitate to serve as the total RNA.

The RNA concentration and purity were determined using a NanoDrop spectrophotometer (Thermo Fisher Scientific). Biotinylated cDNA was prepared from 100 ng of total RNA using the GeneChip WT PLUS Reagent Kit (Thermo Fisher Scientific) following the manufacturer's instructions. Following fragmentation, 2 μg of single-stranded cDNA was hybridized for 16 h at 45°C on Clariom S Mouse. The arrays were washed and stained using GeneChip Fluidics Station 450 (Thermo Fisher Scientific). The Clariom S array was scanned using a GeneChip Scanner 3000 7G. The data were analysed with Expression Console Software 1.4, which offered SST-RMA for gene level analysis using Thermo Fisher Scientific default analysis settings.

Messenger RNA levels in the hippocampus

The hippocampus was homogenized with ISOGEN II (Nippon Gene), and the supernatant was collected. RNA was precipitated with isopropanol, and the precipitate was dried. Thirty microlitres of RNase-free water was added to the RNA precipitate. Reverse transcription was performed using ReverTra Ace qPCR Master Mix with gDNA Remover (Toyobo, Osaka, Japan). Real-time PCR was performed with Mx3000P and Mx3005P (Stratagene, Agilent Technologies, Santa Clara, CA, USA) with 40 cycles using THUNDERBIRD SYBR qPCR Mix (TOYOBO). Sequences of the primers, for Glyceraldehyde-3-phosphate dehydrogenase (*GAPDH*), hemopexin, and lipocalin-2 (*Lcn2*), are as follows:

i *GAPDH* (R): 5′-TTGCTGTTGAAGTCGCAGGAG-3′
ii *GAPDH* (F): 5′-TGTGTCCGTCGTGGATCTGA-3′
iii *Hemopexin* (R): 5′-TGGCAAAGTCCCAGAACCAC-3′
iv *Hemopexin* (F): 5′-TGGAATCCCATACCCACCAGA-3′
v *Lcn2* (R): 5′-GTCTCTGCGCATCCCAGTCA-3′
vi *Lcn2* (F): 5′-GGAACGTTTCACCCGCTTTG-3′

Hemopexin intraventricular administration

Continuous intracerebroventricular (i.c.v.) administration of recombinant hemopexin was performed using a micro-osmotic pump model 1002 (Alzet, Cupertino, CA, USA). This pump delivers the internal solution at a rate of 0.25 μL/h for 14 days. Considering the increased hemopexin levels in the plasma by applying cast and the ratio of transfer of plasma proteins to the brain,[20] concentration of delivery of hemopexin was set to 0.02 mg/mL in the cerebrospinal fluid (CSF). Recombinant hemopexin or distilled water with the artificial CSF [130 mM NaCl, 24 mM $NaHCO_3$, 3.5 mM KCl, 1.3 mM Na_2PO_4, 2 mM $CaCl_2$, 2 mM $MgCl_2{\cdot}6H_2O$, 10 mM glucose, pH 7.4] was filled into the pump. One day prior, the pump was immersed in saline and incubated overnight at 37°C. Wildtype and 5XFAD mice (6–7 weeks old, male and female) were used. After making small hole with an electric microdrill at A/P: −0.2 mm, M/L: +1.0 mm, depth: 3.0 mm, a cannula was inserted and fixed with Aron Alpha (Daiichi Sankyo, Tokyo, Japan). After the surgical operation, antisedan was intraperitoneally administered as an anti-anaesthetic.

Histological analysis

The whole brain was isolated and immediately immersed in 4% paraformaldehyde in PBS. After 8–18 h, the brain was immersed in 30% sucrose for cryoprotection, and the tissue was stored at −30°C. Using a cryostat (CM3050S, Leica, Land hessen, Germany), coronary slices of the brain with a thickness of 12 μm were prepared. To quantify the number of Aβ plaques, slices were stained with 0.01 mg/mL of thioflavin T (FUJIFILM Wako Pure Chemical, Osaka, Japan). The number of Aβ plaques was counted manually. To quantify the expression levels of LCN2, slices were immunostained with a polyclonal antibody against LCN2 (1:60; R&D Systems, Minneapolis, MN, USA). The neurons, microglia, and astrocytes were stained with antibodies against NeuN (1:500, Abcam), Iba1 (1:1000, Wako), and GFAP (1:1000; Merck, Darmstadt, Germany). Alexa Fluor 594-conjugated donkey anti-goat IgG (1:800, Thermo Fisher Scientific), Alexa Fluor 488-conjugated donkey anti-rabbit IgG (1:500, Thermo Fisher Scientific), Alexa Fluor 488-conjugated donkey anti-mouse IgG (1:500, Thermo Fisher Scientific), and Alexa Fluor 647-conjugated donkey anti-rabbit IgG (1:800, Thermo Fisher Scientific) were used as secondary antibodies. The number of positive cells and fluorescent intensity of LCN2 were quantified using ImageJ (National Institutes of Health, Bethesda, MD, USA).

Statistics

Data are expressed as the mean ± standard deviation. For statistical analysis, Prism 5.04 or Prism 7.05 (GraphPad Software, San Diego, CA, USA) was used to perform two-tailed paired *t*-test, one-way analysis of variance with *post hoc* Bonferroni's test, and two-tailed unpaired *t*-test. The significance level was set at 5%.

Results

Cast immobilization accelerates the onset of memory deficit in 5XFAD mice

The time for onset of memory deficits in 5XFAD mice was 16–20 weeks of age. In *Figures* 1 to 3, pre-onset (12–14 weeks of age) 5XFAD mice and age-matched wildtype mice are used. For 5XFAD mice, cast-attached to the hindlimbs and

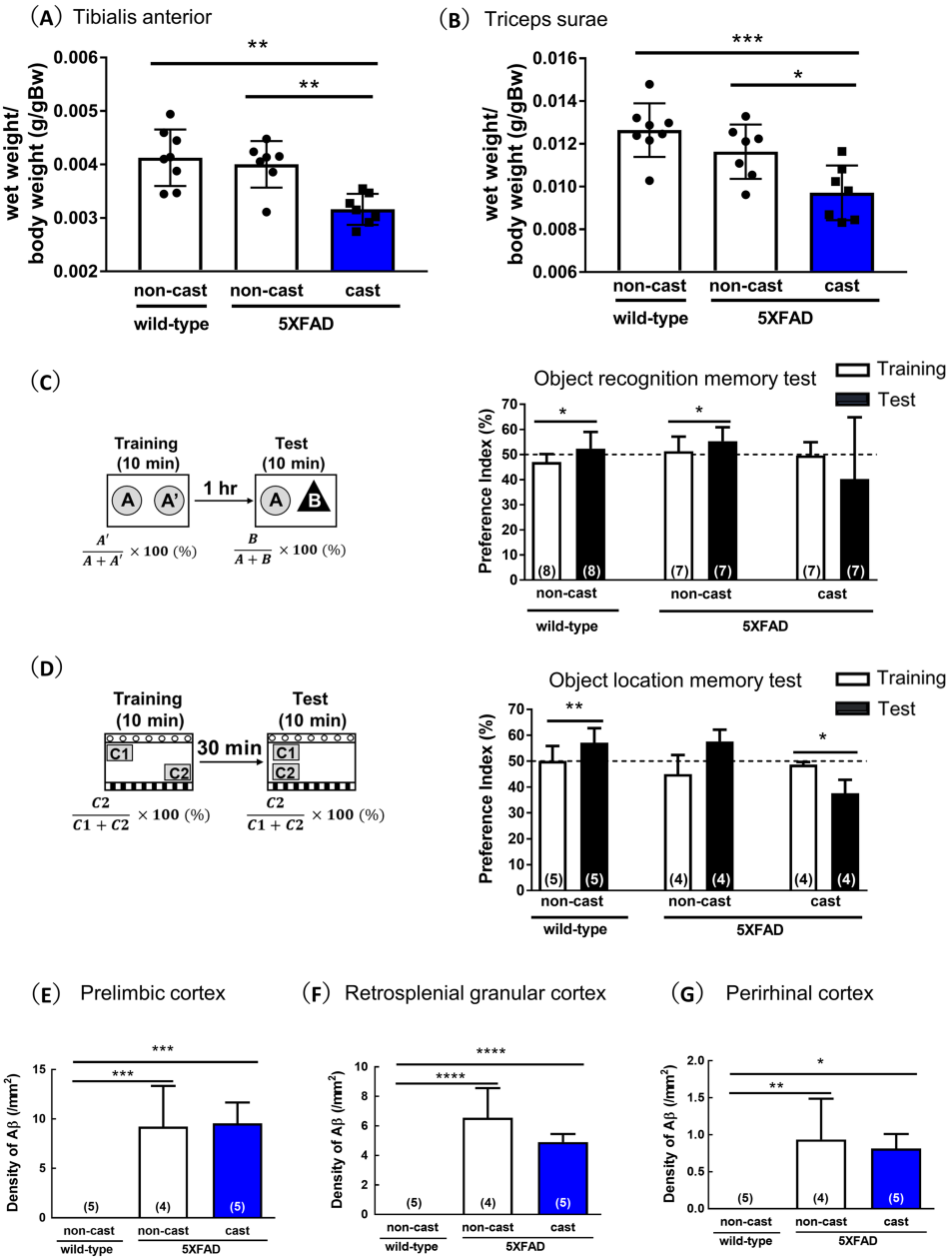

Figure 1 Cast immobilization of the hindlimbs accelerates memory function in pre-onset 5XFAD mice. The 5XFAD mice (12–14 weeks old, male and female) and age-matched wildtype mice are used. The 5XFAD mice are divided into non-cast and cast-attached groups. After two-weeks of casting, the muscle weight and memory function are evaluated. Wet weight of the *(A)* tibialis anterior and *(B)* triceps surae are shown. $^{*}P < 0.05$, $^{**}P < 0.01$, $^{***}P < 0.001$; one-way ANOVA, *post hoc* Bonferroni's test; n = 7–8. *(C)* The object recognition memory test is performed with a 1 h interval between the Training and Test sessions. $^{*}P < 0.05$, two-tailed paired t-test, n = 7–8. *(D)* The object location memory test is performed with a 30 min interval between the Training and Test sessions. $^{*}P < 0.05$, $^{**}P < 0.01$. Two-tailed paired t-test, n = 4–5. (E–G) Amyloid-β (Aβ) plaques in the prelimbic cortex, retrosplenial granular cortex, and perirhinal cortex are measured. One-way ANOVA, *post hoc* Bonferroni's test; n = 4–5. Values are represented as mean ± SD.

non-cast groups were considered. Wildtype mice were non-attached. Two weeks after cast immobilization, the tibialis anterior and triceps surae were excised. Wet weights of the tibialis anterior (*Figure* 1A) and triceps surae (*Figure* 1B) were significantly lower in cast-attached 5XFAD mice than those in non-cast wildtype and 5XFAD mice. After 2 weeks of cast immobilization, memory function was evaluated. In the object recognition test, the PI in the Test session was significantly higher than those in the Training session in non-cast wildtype and 5XFAD mice (*Figure* 1C).

DOI: 10.1002/jcsm.12830

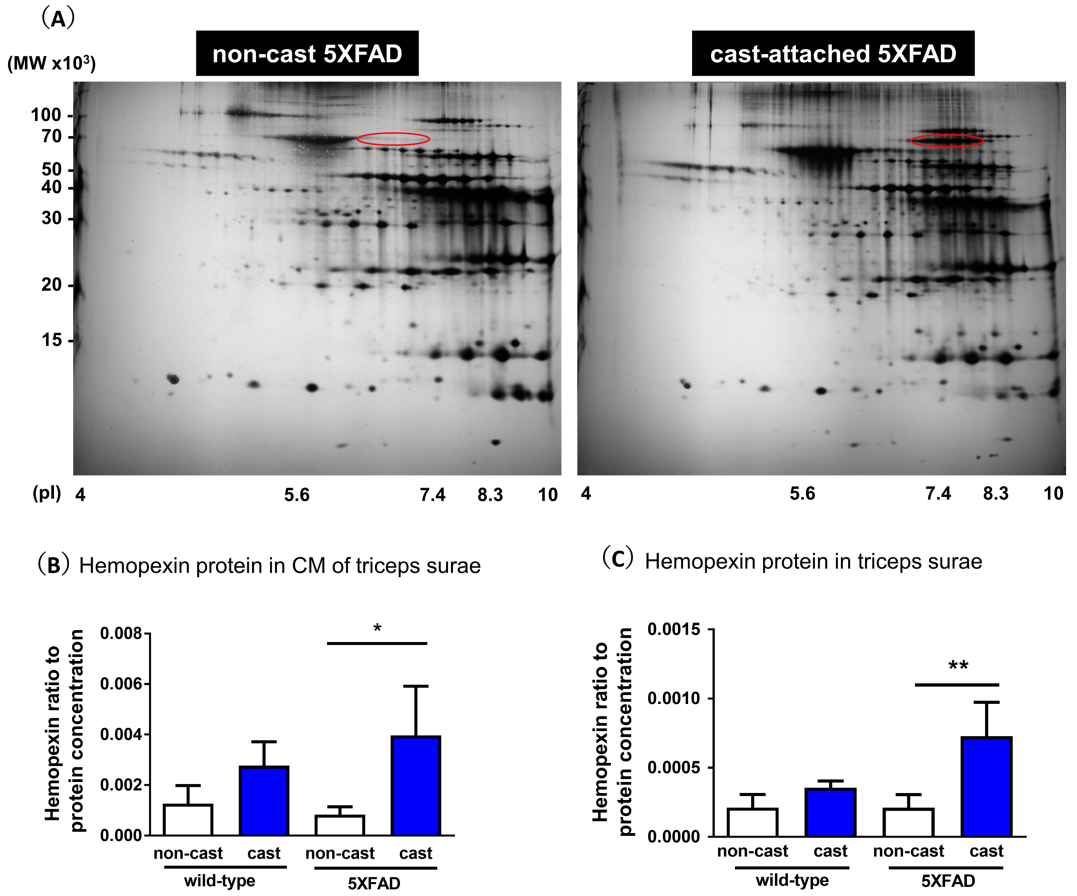

Figure 2 Identification of secreted proteins from the atrophied skeletal muscle. After two-weeks of cast immobilization, the triceps surae are isolated from the pre-onset 5XFAD mice (12–13 weeks old, male). *(A)* Conditioned media (CM) of organ culture of the triceps surae of non-cast 5XFAD and cast-attached 5XFAD mice are loaded on 2D-PAGE. Spots encircled by red lines are the most increased spots in the cast-attached 5XFAD mice, of which hemopexin is identified by matrix-assisted laser desorption/ionization-time-of-flight mass spectrometry MALDI-TOF MS. *(B)* Pre-onset 5XFAD mice and age-matched wildtype mice are either cast-attached or not for 2 weeks. The isolated triceps surae are cultured for 24 h, and the CM are collected. The concentration of hemopexin in the CM is quantified by ELISA. $*P < 0.05$; one-way ANOVA, *post hoc* Bonferroni's test; $n = 3$. *(C)* The concentration of hemopexin in the triceps surae is quantified by ELISA. $**P < 0.01$; one-way ANOVA, *post hoc* Bonferroni's test; $n = 3$. Values are represented as mean ± SD.

In contrast, cast-attached 5XFAD mice showed no increase in the PI in the Training session (*Figure* 1C), indicating memory deficits. A similar result was also obtained in the object location memory test, which evaluated spatial memory (*Figure* 1D). Cast immobilization disrupted the memory function for both the object and location in pre-onset 5XFAD mice.

Aβ deposition in the brain was evaluated by Aβ-specific staining using thioflavin T. As reported previously, Aβ plaques were detected in several brain regions even in pre-onset 5XFAD mice, such as the prelimbic cortex (*Figure* 1E), retrosplenial granular cortex (*Figure* 1F), and perirhinal cortex (*Figure* 1G). In these areas, the elevated Aβ levels in 5XFAD mice remained unchanged by cast immobilization.

Hemopexin is secreted from the atrophied skeletal muscle

To explore proteins secreted from the atrophied skeletal muscle in cast-attached 5XFAD mice, a comparison of CM in 2D-PAGE was performed. The triceps surae were isolated from non-cast and cast-attached 5XFAD mice and used for organ culture. After incubating for 24 h, culture media were collected as CM and compared to identify differentially expressed proteins. In total, 88 spots were detected as increased in the cast-attached muscle-derived CM than that in non-cast muscle-derived CM (*Figure* 2A). The most increased protein in the cast-attached muscle-derived CM was identified as hemopexin by matrix-assisted laser desorption/ionization-time-of-flight mass spectrometry analysis

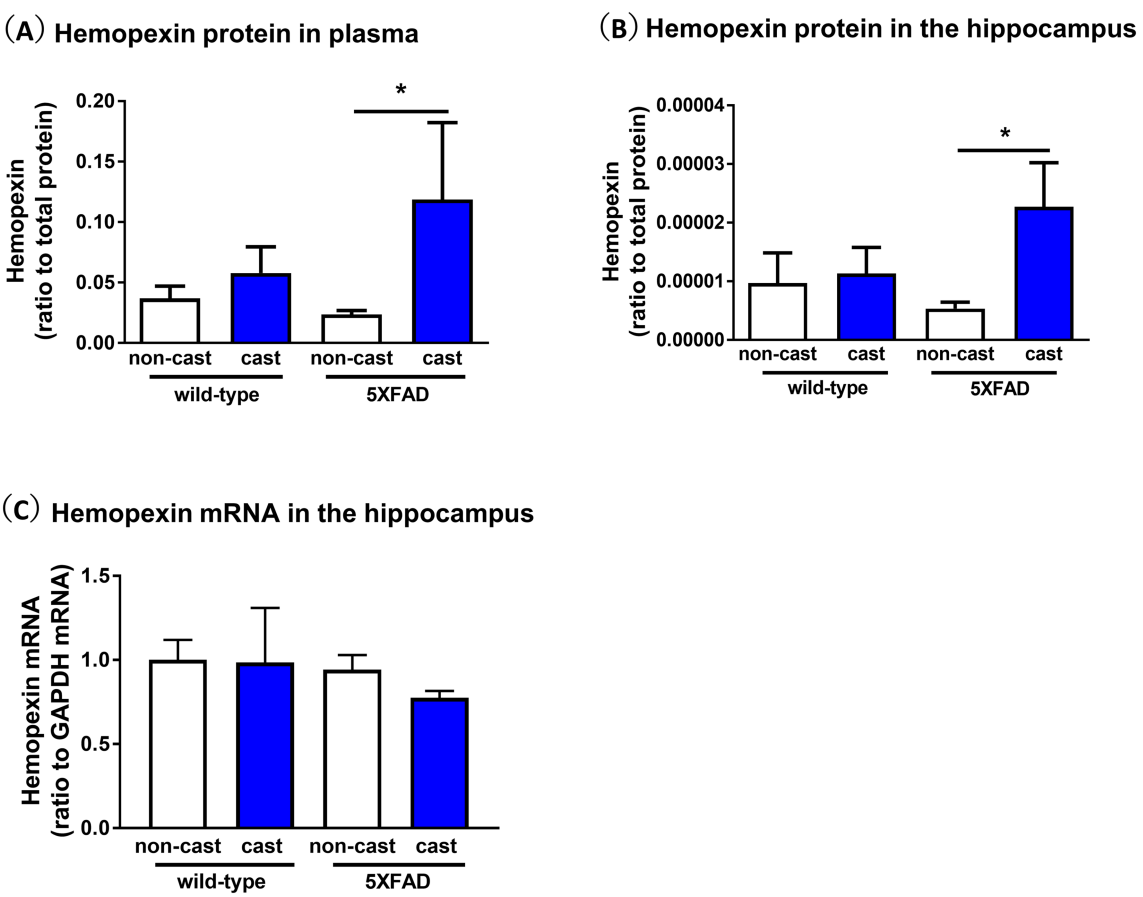

Figure 3 Concentration of hemopexin in the plasma and hippocampus. Pre-onset 5XFAD mice (11–13 weeks old, male) and age-matched wildtype mice are either cast-attached or not for two-weeks. *(A)* The concentration of hemopexin in the plasma is quantified by ELISA. *$P < 0.05$; one-way ANOVA, *post hoc* Bonferroni's test; $n = 3$. *(B)* The concentration of hemopexin in the hippocampus is quantified by ELISA. *$P < 0.05$; one-way ANOVA, *post hoc* Bonferroni's test; $n = 3$. *(C)* Expression levels of hemopexin mRNA with respect to those of *GAPDH* mRNA; $n = 3$. Values are represented as mean ± SD.

Table 1 Summary of presented data in this study

	Pre-symptomatic 5XFAD mouse	
	Cast (vs. non-cast)	Hemopexin i.c.v. infusion (vs. vehicle)
Skeletal muscle wet weight	Decrease**	No need to check
Memory	Deficit	Deficit
Aβ plaque	No change	Not detected
Protein level of hemopexin in CM of organ cultured muscle	Increase*	No need to check
Protein level of hemopexin in skeletal muscle lysate	Increase**	No need to check
Protein level of hemopexin in plasma	Increase*	No need to check
Protein level of hemopexin in hippocampus	Increase*	—
Hemopexin mRNA in hippocampus	No change	—
Protein level of LCN2 in hippocampus	Increase*	—
Lcn2 mRNA in hippocampus	Increase*	Increase

'—', not determined
*$P < 0.05$,
**$P < 0.01$.

(score: 215, coverage: 43). Hemopexin levels in CM from the non-cast and cast-attached wildtype and 5XFAD mice were investigated by ELISA (*Figure* 2B). The hemopexin level in the CM from cast-attached 5XFAD muscles was significantly higher than that in CM from non-cast 5XFAD muscles. After organ culture, the triceps surae were homogenized and used for ELISA. The expression of hemopexin in the triceps surae was significantly increased in the cast-attached 5XFAD

muscles than that in non-cast 5XFAD muscles (*Figure* 2C). Moreover, in wildtype mice, cast immobilization tended to increase the levels of hemopexin in the triceps surae (*Figure* 2C) and CM (*Figure* 2B).

Hemopexin reaches the brain via blood circulation

We presumed that the hemopexin secreted from the skeletal muscles may be transferred to the brain via systemic circulation. To address this question, hemopexin protein levels in the blood and brain were quantified by ELISA. The hemopexin concentration in the plasma of cast-attached 5XFAD mice was significantly higher than that in the plasma of non-cast 5XFAD mice (*Figure* 3A). The hemopexin protein concentration in the hippocampus of cast-attached 5XFAD mice was significantly higher than that in the hippocampus of non-cast 5XFAD mice (*Figure* 3B). The levels of hemopexin messenger RNA (mRNA) in the hippocampus quantified by real-time PCR showed no differences in the four groups (*Figure* 3C). Therefore, the cast immobilization-induced increase in hemopexin levels in the hippocampus was not mediated by transcriptional up-regulation in the hippocampus, but possibly due to stimulus from the muscles.

Intracerebroventricular infusion of recombinant hemopexin induces memory impairment in pre-onset 5XFAD mice

We evaluated the effects of increased hemopexin on memory function. Recombinant hemopexin protein was continuously administered by i.c.v. infusion for 2 weeks, and the object recognition memory test was performed using pre-onset 5XFAD mice (8–9 weeks old, male and female) and age-matched wildtype mice. In both wildtype and 5XFAD mice, vehicle solution-administered groups showed significantly higher PI in the Test session than in hemopexin-administered groups (*Figure* 4). However, the recombinant hemopexin-administered groups showed no difference in PI between the Training and Test sessions, indicating acceleration of memory deficit by hemopexin infusion in the brain. Thioflavin stained Aβ deposition in the brain was not detected in all animals, maybe due to too young age (data not shown).

Treatment with hemopexin up-regulates expression of lipocalin-2 in the brain

Hemopexin-induced memory dysfunction has not yet been reported. Therefore, it is unknown why hemopexin

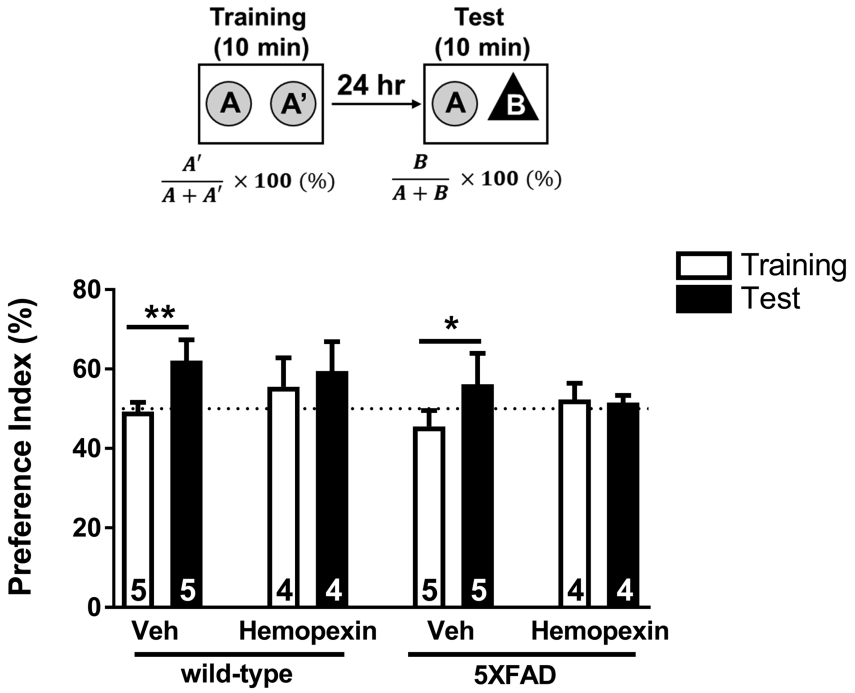

Figure 4 Intracerebroventricular (i.c.v.) infusion of hemopexin accelerates memory deficit in pre-onset 5XFAD mice. The 5XFAD mice (6–7 weeks old, male and female) and age-matched wildtype mice are used. Recombinant hemopexin or vehicle solution is continuously i.c.v. infused for 2 weeks. Object recognition memory test is performed with a 24 h interval between the Training and Test sessions. *$P < 0.05$, **$P < 0.01$; two-tailed paired *t*-test; n = 4–5. Values are represented as mean ± SD.

accelerates memory deficits. To identify the hemopexin-induced events in the hippocampus, a comprehensive comparison of mRNA was performed by gene microarray, which covered 22 206 genes. Pre-onset 5XFAD mice (6–7 weeks old, male and female) were i.c.v. infused with recombinant hemopexin for 2 weeks. The hippocampus was isolated from recombinant hemopexin-infused and vehicle-infused 5XFAD mice. The samples from hemopexin-infused mice showed 116 up-regulated genes (Supporting Information, *Table* S1) and 155 down-regulated genes (*Table* S2) than those from vehicle-infused 5XFAD mice. We focused on lipocalin-2 (Lcn2) because its increase

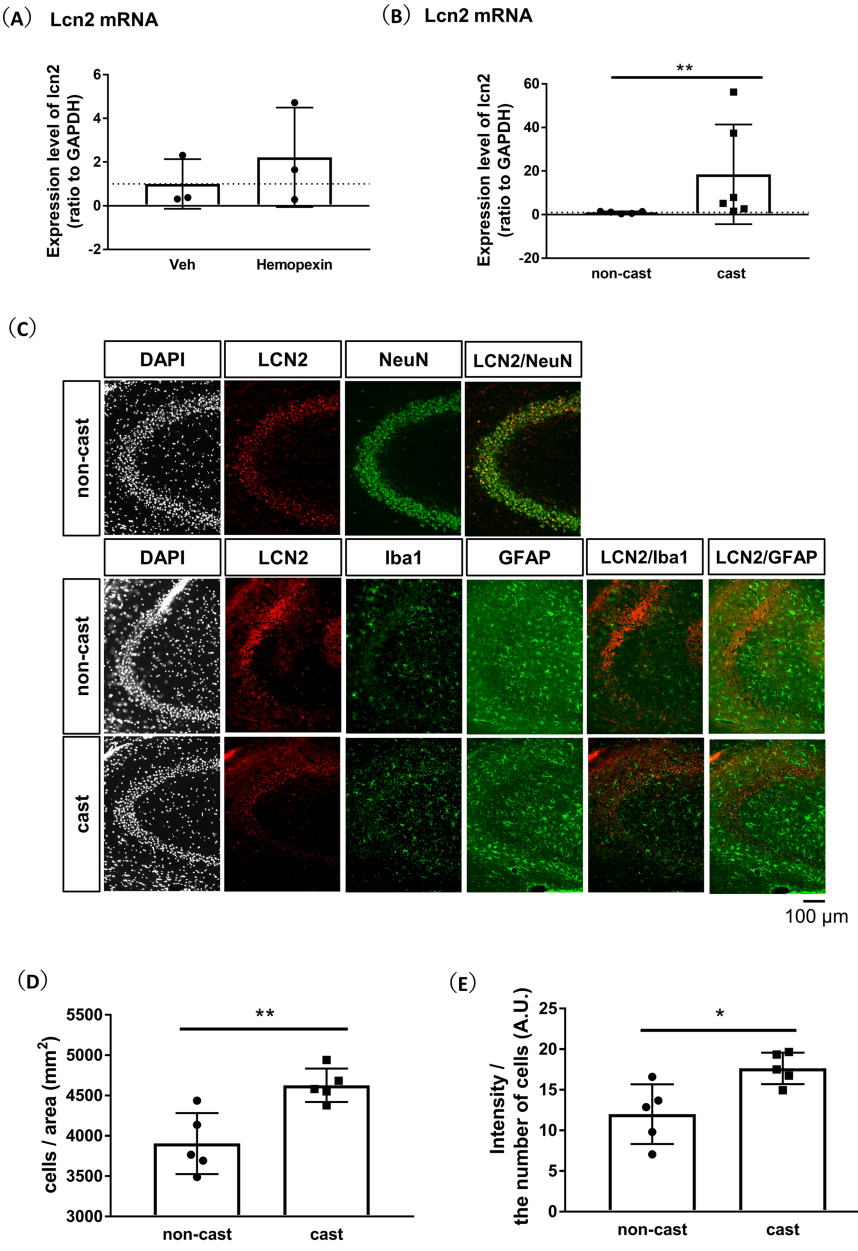

Figure 5 Expression of lipocalin-2 is increased in the hippocampus by intracerebroventricular (i.c.v.) infusion of hemopexin as well as cast-immobilization. *(A)* The 5XFAD mice (6–7 weeks old, male and female) are used. Recombinant hemopexin or vehicle solution is continuously i.c.v. infused for 2 weeks. The expression of *Lcn2* mRNA in the hippocampus is quantified; $n = 3$. *(B)* The 5XFAD mice (11–14 weeks old, male) are used. The hindlimbs are immobilized by casting for 2 weeks. The expression of *Lcn2* mRNA in the hippocampus is quantified; $n = 5$–6. $^{**}P < 0.01$; two-tailed *t*-test; $n = 5$–6. *(C)* The 5XFAD mice (11–14 weeks old, male and female) are used. The hindlimbs are immobilized by casting for 2 weeks. Representative immunostaining of LCN2, NeuN, GFAP, and Iba1 in the hippocampal CA3 is shown. DAPI is used for counterstaining the nuclei. Scale, 100 μm. *(D)* LCN2-positive cell numbers in the hippocampal CA3 region. $^{**}P < 0.01$; two-tailed *t*-test; $n = 5$. *(E)* Intensity of LCN2 expression in the hippocampal CA3 region. $^{*}P < 0.05$; two-tailed *t*-test; $n = 5$. Values are represented as mean ± SD.

DOI: 10.1002/jcsm.12830

was top ranked. The increase in Lcn2 levels in the hippocampus was confirmed using real-time PCR. The hippocampus in recombinant hemopexin-infused 5XFAD mice showed high expression of Lcn2 mRNA than that in vehicle-infused 5XFAD mice (*Figure* 5A). Pre-onset 5XFAD mice (11–14 weeks old, male) were either cast-attached or not for two-weeks. The hippocampal Lcn2 mRNA levels were significantly increased in cast-immobilized 5XFAD mice than those in non-cast mice (*Figure* 5B).

Immunohistochemistry was performed to evaluate the protein expression levels of LCN2. LCN2 was detected in the hippocampus, and the LCN2-positive signal completely merged with NeuN-positive neuronal cell bodies, but not GFAP-positive astrocytes or Iba1-positive microglia (*Figure* 5C). In the CA3 region, the number of LCN2-positive neurons (*Figure* 5D) and intensity of expression of LCN2 (*Figure* 5E) were significantly increased in the cast-attached 5XFAD mice than that in non-cast 5XFAD mice.

Discussion

This study revealed that the disuse-induced skeletal muscle atrophy shifted the onset of memory dysfunction earlier without increasing the deposition of Aβ in young mice model of AD. The atrophied muscles secreted hemopexin, and hemopexin was transported to the brain, possibly via systemic circulation. Moreover, increased levels of hemopexin in the brain or cast immobilization-induced muscle atrophy similarly impaired memory function and elevated the expression of LCN2 in the hippocampal CA3 neurons. Additionally, LCN2, a hemopexin-induced protein in the present study, is known to be crucially associated with neuroinflammation. Therefore, these findings indicate that the skeletal muscle atrophy has an unbeneficial impact on the occurrence of memory impairment in young mice, which is mediated by the muscle-origin hemopexin and hemopexin-driven neuroinflammation.

Hemopexin, a glycoprotein with a molecular weight of approximately 57 000 Da, is abundant in the blood. Hemopexin is primarily synthesized in the liver, and its basic function is to bind to heme, leading to reduced heme toxicity. As the secretion of hemopexin from the skeletal muscle has not been studied previously, the mechanisms of synthesis and secretion remain unknown. In the H-35 hepatoma cells, treatment with IL-6 stimulates the transcription of hemopexin.[21] Therefore, we hypothesized that skeletal muscle atrophy may increase expression of IL-6 and up-regulate hemopexin transcription in the muscle, as IL-6 is a key regulator of protein degradation in the muscles.[22]

To date, the beneficial effects of hemopexin on neuronal function have been reported. For example, i.c.v. administration of hemopexin in cerebral ischemic rats reduced the infarct volumes and improved the measurements of neurological function.[23] Hemopexin-null mice show hypomyelination in the brain.[24] However, a recent clinical study reported unbeneficial effects of hemopexin in the brain, where higher levels of hemopexin associated with progression of AD pathology, and hemopexin was negatively associated with cognitive score.[25] The concentration of hemopexin in the CSF is higher in patients with AD than in normal subjects.[26] The basal synthesis of hemopexin in the brain is primarily restricted to the ventricular ependymal cells, and other cell types, such as neurons, only scarcely synthesize hemopexin. Therefore, transport of hemopexin from the skeletal muscles may boost the elevated levels of hemopexin in the brain. We hypothesize that hemopexin of the skeletal muscle-origin is delivered to the brain in a form distinguishable from hemopexin of liver-origin; for example, exosome-mediated delivery from the skeletal muscles. This possibility is currently under investigation at our laboratory.

So far, clinical studies showed that sarcopenia and cognitive decline are correlated. However, it has not indicated what is a trigger of the sarcopenia-induced cognitive decline because it is hard to distinguish skeletal muscle atrophy-triggered events and other events in case of using aged animals and subjects. Therefore, this study gave a pinpoint intervention, cast-induced muscle-atrophy, and revealed that the skeletal muscle atrophy elicited cognitive impairment. Responsible molecular of the events is skeletal muscle-origin hemopexin that travels to the brain.

The levels of *Lcn2* were increased in the hippocampus by cast immobilization and hemopexin i.c.v. infusion, individually. LCN2 is a glycoprotein with a molecular weight of approximately 25 000 and is known to promote neuroinflammation via recruitment and activation of the glial cells.[27] Overexpression of *Lcn2* in the astrocytes increases expression of iNOS and aggravates injury, which is reversed by knockout of *Lcn2*.[28] In the hippocampus, LCN2 is primarily expressed in the neurons and is only weakly expressed in astrocytes and microglia,[29] corroborating the observations of the present study. Therefore, the increase in levels of LCN2 in the neurons appears to directly deteriorate neuroinflammation. A recent study identified high expression of LCN2 in the brains in individuals with AD during postmortem,[30] as well as in individuals with mild cognitive impairment.[31] Therefore, we are currently investigating the mechanism by which hemopexin promotes expression of Lcn2 in the neurons.

Our study has several limitations. First, although this study used 5XFAD mice as an AD model, other AD models also need to be investigated. Second, induction mechanisms of LCN2 mRNA in the hippocampus by hemopexin i.c.v. infusion or cast-attachment remain unknown. Third, concrete phenomena of neuroinflammation via LCN2 are not confirmed. Finally, protein level of LCN2 in the hippocampus was not investigated in hemopexin i.c.v. infused mice.

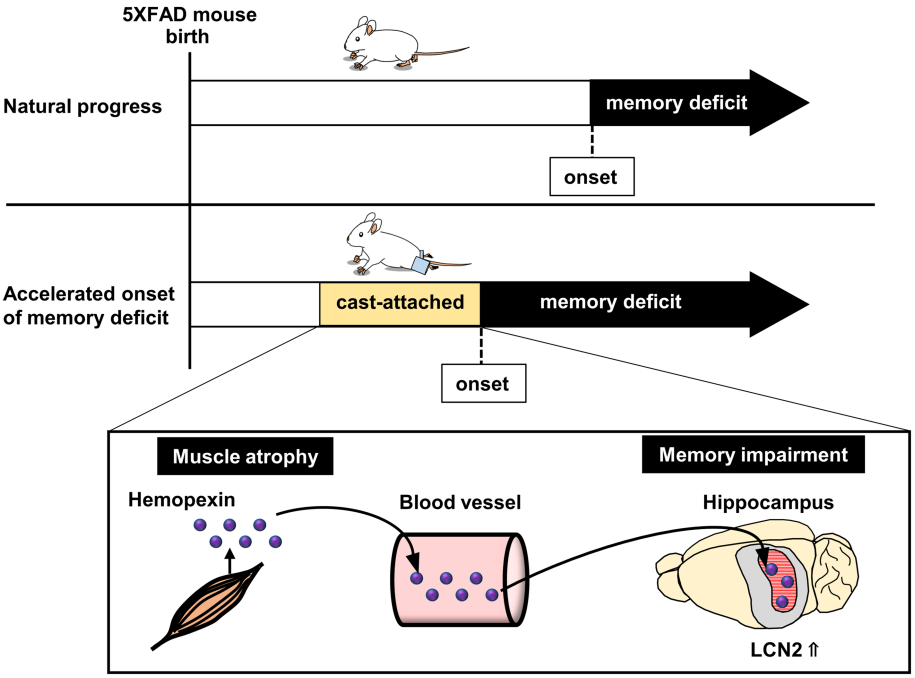

Figure 6 Summary of the study.

In conclusion, this is the first study to describe that the skeletal muscle atrophy shifts the onset of memory deficits earlier via secretion of hemopexin using a mouse model of AD (*Figure* 6). Thus, protecting the brain from secretion of hemopexin from the skeletal muscles and/or inhibiting hemopexin signalling in the neurons could be a new approach for the prevention of AD.

Acknowledgements

The authors certify that they comply with the ethical guidelines for authorship and publishing in the *Journal of Cachexia, Sarcopinia, and Muscle*.[32] We would like to thank Editage for editing this manuscript for English language.

Conflict of interest

Tsukasa Nagase and Chihiro Tohda declare that they have no conflicts of interest.

Funding

This study was supported by the discretionary funds of the President of the University of Toyama in 2019–2020.

Author contribution

Nagase T and Tohda C designed the experiments. Nagase T performed all the experiments and analyses. Nagase T and Tohda C wrote the manuscript. Tohda C supervised the study.

Ethical standards

The manuscript does not contain clinical studies or patient data.

Online supplementary material

Additional supporting information may be found online in the Supporting Information section at the end of the article.

Table S1. increased gene expression in 5XFAD mouse hippocampus after hemopexin i.c.v. infusion.

Table S2. decreased gene expression in 5XFAD mouse hippocampus after hemopexin i.c.v. infusion.

References

1. Ashrafian H, Zadeh EH, Khan RH. Review on Alzheimer's disease: inhibition of amyloid beta and tau tangle formation. *Int J Biol Macromol* 2021;**167**:382–394.
2. Huang LK, Chao SP, Hu CJ. Clinical trials of new drugs for Alzheimer disease. *J Biomed Sci* 2020;**27**:18.
3. Decourt B, Boumelhem F, Pope ED 3rd, Shi J, Mari Z, Sabbagh MN. Critical appraisal of amyloid lowering agents in AD. *Curr Neurol Neurosci Rep* 2021;**21**:39.
4. Aizenstein HJ, Nebes RD, Saxton JA, Price JC, Mathis CA, Tsopelas ND, et al. Frequent amyloid deposition without significant cognitive impairment among the elderly. *Arch Neurol* 2008;**65**:1509–1517.
5. Johnson KA, Minoshima S, Bohnen NI, Donohoe KJ, Foster NL, Herscovitch P, et al. Update on appropriate use criteria for amyloid PET imaging: dementia experts, mild cognitive impairment, and education. Amyloid Imaging Task Force of the Alzheimer's Association and Society for Nuclear Medicine and Molecular Imaging. *Alzheimers Dement* 2013;**9**: e106–e109.
6. Ossenkoppele R, Jansen WJ, Rabinovici GD, Knol DL, van der Flier WM, van Berckel BN, et al. Prevalence of amyloid PET positivity in dementia syndromes: a meta-analysis. *JAMA* 2015;**313**:1939–1949.
7. Roberts RO, Aakre JA, Kremers WK, Vassilaki M, Knopman DS, Mielke MM, et al. Prevalence and outcomes of amyloid positivity among persons without dementia in a longitudinal, population-based setting. *JAMA Neurol* 2018;**75**:970–979.
8. Barnes DE, Yaffe K. The projected effect of risk factor reduction on Alzheimer's disease prevalence. *Lancet Neurol* 2011;**10**: 819–828.
9. Hsu YH, Liang CK, Chou MY, Liao MC, Lin YT, Chen LK, et al. Association of cognitive impairment, depressive symptoms and sarcopenia among healthy older men in the veterans retirement community in southern Taiwan: a cross-sectional study. *Geriatr Gerontol Int* 2014;**14**:102–108.
10. Peng TC, Chen WL, Wu LW, Chang YW, Kao TW. Sarcopenia and cognitive impairment: a systematic review and meta-analysis. *Clin Nutr* 2020;**39**:2695–2701.
11. Maeda K, Akagi J. Cognitive impairment is independently associated with definitive and possible sarcopenia in hospitalized older adults: the prevalence and impact of comorbidities. *Geriatr Gerontol Int* 2017;**17**:1048–1056.
12. Bickel H, Hendlmeier I, Heßler JB, Junge MN, Leonhardt-Achilles S, Weber J, et al. The prevalence of dementia and cognitive impairment in hospitals. *Dtsch Arztebl Int* 2018;**115**:733–740.
13. Benatti FB, Pedersen BK. Exercise as an anti-inflammatory therapy for rheumatic diseases-myokine regulation. *Nat Rev Rheumatol* 2015;**11**:86–97.
14. Pedersen BK, Febbraio MA. Muscles, exercise and obesity: skeletal muscle as a secretory organ. *Nat Rev Endocrinol* 2012;**8**:457–465.
15. Kim S, Choi JY, Moon S, Park DH, Kwak HB, Kang JH. Roles of myokines in exercise-induced improvement of neuropsychiatric function. *Pflugers Arch* 2019;**471**:491–505.
16. Delezie J, Handschin C. Endocrine crosstalk between skeletal muscle and the brain. *Front Neurol* 2018;**9**:698.
17. Valenzuela PL, Castillo-García A, Morales JS, de la Villa P, Hampel H, Emanuele E, et al. Exercise benefits on Alzheimer's disease: state-of-the-science. *Ageing Res Rev* 2020;**62**:101108.
18. Oakley H, Cole SL, Logan S, Maus E, Shao P, Craft J, et al. Intraneuronal beta-amyloid aggregates, neurodegeneration, and neuron loss in transgenic mice with five familial Alzheimer's disease mutations: potential factors in amyloid plaque formation. *J Neurosci* 2006;**26**:10129–10140.
19. Kimbara Y, Shimada Y, Kuboyama T, Tohda C. *Cistanche tubulosa* (Schenk) Wight extract enhances hindlimb performance and attenuates myosin heavy chain IId/IIx expression in cast-immobilized mice. *Evid Based Complement Alternat Med* 2019;**2019**:9283171.
20. Liddelow SA, Dzięgielewska KM, Møllgård K, Whish SC, Noor NM, Wheaton BJ, et al. Cellular specificity of the blood-CSF barrier for albumin transfer across the choroid plexus epithelium. *PLoS ONE* 2014;**9**:e106592.
21. Immenschuh S, Nagae Y, Satoh H, Baumann H, Muller-Eberhard U. The rat and human hemopexin genes contain an identical interleukin-6 response element that is not a target of CAAT enhancer-binding protein isoforms. *J Biol Chem* 1994;**269**:12654–12661.
22. Webster JM, Kempen LJAP, Hardy RS, Langen RCJ. Inflammation and skeletal muscle wasting during cachexia. *Front Physiol* 2020;**11**:597675.
23. Dong B, Yang Y, Zhang Z, Xie K, Su L, Yu Y. Hemopexin alleviates cognitive dysfunction after focal cerebral ischemia-reperfusion injury in rats. *BMC Anesthesiol* 2019;**19**:13.
24. Morello N, Bianchi FT, Marmiroli P, Tonoli E, Rodriguez Menendez V, Silengo L, et al. A role for hemopexin in oligodendrocyte differentiation and myelin formation. *PLoS ONE* 2011;**6**:e20173.
25. Ashraf AA, Dani M, So PW. Low cerebrospinal fluid levels of hemopexin are associated with increased Alzheimer's pathology, hippocampal hypometabolism, and cognitive decline. *Front Mol Biosci* 2020;**7**:590979.
26. Ringman JM, Schulman H, Becker C, Jones T, Bai Y, Immermann F, et al. Proteomic changes in cerebrospinal fluid of presymptomatic and affected persons carrying familial Alzheimer disease mutations. *Arch Neurol* 2012;**69**:96–104.
27. Lim D, Jeong JH, Song J. Lipocalin 2 regulates iron homeostasis, neuroinflammation, and insulin resistance in the brains of patients with dementia: evidence from the current literature. *CNS Neurosci Ther* 2021;**00**:1–12.
28. Zhao N, Xu X, Jiang Y, Gao J, Wang F, Xu X, et al. Lipocalin-2 may produce damaging effect after cerebral ischemia by inducing astrocytes classical activation. *J Neuroinflammation* 2019;**16**:168.
29. Furukawa T, Shimoyama S, Miki Y, Nikaido Y, Koga K, Nakamura K, et al. Chronic diazepam administration increases the expression of Lcn2 in the CNS. *Pharmacol Res Perspect* 2017;**5**:e00283.
30. Naudé PJ, Nyakas C, Eiden LE, Ait-Ali D, van der Heide R, Engelborghs S, et al. Lipocalin 2: novel component of proinflammatory signaling in Alzheimer's disease. *FASEB J* 2012;**26**:2811–2823.
31. Choi J, Lee HW, Suk K. Increased plasma levels of lipocalin 2 in mild cognitive impairment. *J Neurol Sci* 2011;**305**:28–33.
32. von Haehling S, Morley JE, Coats AJS, Anker SD. Ethical guidelines for publishing in the Journal of Cachexia, Sarcopenia and Muscle: update 2019. *J Cachexia Sarcopenia Muscle* 2019;**10**:1143–1145.